Trace gas and aerosol interactions in the fully coupled model of aerosol-chemistry-climate ECHAM5-HAMMOZ: 2. Impact of heterogeneous chemistry on the global aerosol distributions

L. Pozzoli,[1,2] I. Bey,[1] S. Rast,[3] M. G. Schultz,[4] P. Stier,[5,6] and J. Feichter[3]

Received 25 May 2007; revised 31 October 2007; accepted 19 December 2007; published 15 April 2008.

[1] We use the ECHAM5-HAMMOZ aerosol-chemistry-climate model to quantify the influence of trace gas–aerosol interactions on the regional and global distributions and optical properties of aerosols for present-day conditions. The model includes fully interactive simulations of gas phase and aerosol chemistry including a comprehensive set of heterogeneous reactions. We find that as a whole, the heterogeneous reactions have only a small effect on the SO_2 and sulfate burden because of competing effects. The uptake of SO_2 on dust and sea salt decreases the SO_2 concentrations while the decrease in OH (that results from the uptake of HO_2, N_2O_5, and O_3) tends to increase SO_2 (because of reduced oxidation). The sulfate formed in sea salt aerosols from SO_2 uptake accounts for 3.7 Tg(S) a^{-1} (5%) of the total sulfate production. Uptake and subsequent reaction of SO_2 on mineral dust contributes to a small formation of sulfate (0.55 Tg(S) a^{-1}, <1%), but is responsible for the coating of mineral dust particles, resulting in an extra 300 Tg a^{-1} of dust being transferred from the insoluble to the soluble mixed modes. The burden of dust in the insoluble modes is reduced by 44%, while the total burden is reduced by 5% as a result of enhanced wet deposition efficiency. Changes in the sulfur cycle affect the H_2SO_4 concentrations and the condensation of H_2SO_4 on black carbon. Accounting for heterogeneous reactions enhances the global mean burden of hydrophobic black carbon particles by 4%. The changes in aerosol mixing state result only in a small change in the global and annual aerosol optical depth (AOD) and absorption optical depth (ABS), but have significant implications on regional and seasonal scale. For example, in the main polluted regions of the Northern Hemisphere, AOD and ABS increase by 10–30% and up to 15%, respectively, in winter.

Citation: Pozzoli, L., I. Bey, S. Rast, M. G. Schultz, P. Stier, and J. Feichter (2008), Trace gas and aerosol interactions in the fully coupled model of aerosol-chemistry-climate ECHAM5-HAMMOZ: 2. Impact of heterogeneous chemistry on the global aerosol distributions, *J. Geophys. Res.*, *113*, D07309, doi:10.1029/2007JD009008.

1. Introduction

[2] Atmospheric trace gases and aerosols interact in many ways. Many trace gases are precursors of aerosols while aerosols alter the photolysis rates and act as sites for heterogeneous conversion of trace gases. The influence of trace gas–aerosol interactions on trace gas distributions has been discussed in several papers [e.g., *Martin et al.*, 2003; *Tie et al.*, 2005; *Liao and Seinfeld*, 2005; *Pozzoli et al.*, 2008]. These studies suggest that trace gas–aerosol interactions (and in particular heterogeneous reactions) significantly decrease the global O_3 burden and surface O_3 concentrations as well as the global OH burden. Less attention has been paid so far to the influence of trace gas–aerosol interactions on the global distributions and optical properties of aerosols. Trace gas–aerosol interactions may be especially important for the sulfur chemistry. Sulfur dioxide (SO_2) and dimethylsulfide (DMS) are precursors of sulfuric acid (H_2SO_4) which can condense on existing aerosol particles to form sulfate (SO_4^{2-}) or can nucleate to form new ultrafine sulfate particles. It has been suggested that the uptake of SO_2 onto aerosol surfaces such

[1]Laboratoire de Modélisation de la Chimie Atmosphérique, École Polytechnique Fédérale de Lausanne, Lausanne, Switzerland.
[2]Now at Atmosphere in Earth System, Max Planck Institute for Meteorology, Hamburg, Germany.
[3]Atmosphere in Earth System, Max Planck Institute for Meteorology, Hamburg, Germany.
[4]Institute of Chemistry and Dynamics of the Geosphere: Troposphere, Forschungzentrum, Jülich, Germany.
[5]Department of Environmental Science and Engineering, California Institute of Technology, Pasadena, California, USA.
[6]Now at Atmospheric, Oceanic and Planetary Physics, University of Oxford, Oxford, UK.

0148-0227/08/2007JD009008

Table 1. Description of the Aerosol Modes With the Dimensional Size Ranges of the Number Median Radii (r) and the Components Used in HAM Together With the Acronyms Used in the Text[a]

	Soluble/Mixed		Insoluble	
Mode	Label	Component	Label	Component
Nucleation ($r \leq 0.005$ μm)	NS	SU		
Aitken ($0.005 < r \leq 0.05$ μm)	KS	SU, BC, OC	KI	BC, OC
Accumulation ($0.05 < r \leq 0.5$ μm)	AS	SU, BC, OC, SS, DU	AI	DU
Coarse ($r > 0.5$ μm)	CS	SU, BC, OC, SS, DU	CI	DU

[a]SU stands for sulfate, BC stands for black carbon, OC stands for organic carbon, SS stands for sea salt and DU stands for mineral dust. NS stands for nucleation soluble mode, KS stands for Aitken soluble, AS stands for accumulation soluble, CS stands for coarse soluble, KI stands for Aitken insoluble, AI stands for accumulation insoluble, and CI stands for coarse insoluble.

as sea salt and mineral dust can also lead to the formation of sulfate [*Usher et al.*, 2002; *Ullerstam et al.*, 2002; *Song and Carmichael*, 2001; *Alexander et al.*, 2005]. This additional sulfate formation on preexisting particles is an important process as it can change the hygroscopicity of the particles and thus their optical properties and lifetime [e.g., *Ackerman and Toon*, 1981; *Chylek et al.*, 1995; *Jacobson*, 2000; *Koch*, 2001; *Riemer et al.*, 2004; *Croft et al.*, 2005]. The interactions between sulfur compounds in the gas phase and aerosols are still highly uncertain. A key parameter is the uptake coefficient of SO_2 on mineral dust that can vary by several orders of magnitude in the literature (from 10^{-1}–10^{-4} [*Dentener et al.*, 1996] to 10^{-4}–10^{-7} [*Bauer and Koch*, 2005]). The sulfate formation on dust, in sea salt particles, and in cloud droplets depends on the alkalinity of the particles which is only poorly known. The aerosol ageing process is also highly uncertain, and different assumptions can be made to represent the quantity of sulfate needed to coat a dust particle and modify its hygroscopicity.

[3] The global budget of sulfate and sulfur species has been discussed in a number of modeling studies [*Langner and Rodhe*, 1991; *Feichter et al.*, 1996; *Chin et al.*, 1996; *Roelofs et al.*, 1998; *Lohmann et al.*, 1999; *Rasch et al.*, 2000; *Liao and Seinfeld*, 2005; *Bauer and Koch*, 2005; *Alexander et al.*, 2005; *Bell et al.*, 2005]. However, most of these did not include trace gas–aerosol interactions in a comprehensive way; for example off-line fields were used for trace gas oxidants and heterogeneous reactions were not considered, nor the different aerosol species were considered to be externally mixed. *Bauer and Koch* [2005] examined the effect of accounting for the sulfate formation on mineral dust particles. They included the coating of particle surface in their model as well as the changes from hydrophobic to hydrophilic particles; however they used prescribed O_3 fields and only considered sulfate formation on dust particles. *Liao et al.* [2004] used a global model of trace gas–aerosol chemistry in which the heterogeneous reaction of SO_2 on both mineral dust and sea salt is accounted for and found that sulfate formed on these particles contributes significantly (26%) to the global sulfate budget. *Alexander et al.* [2005] constrained their global model with field measurements and showed that formation of sulfate in sea salt particles is a significant but small term in the global sulfur budget (9%).

[4] This paper is the second of a two-part series which examines the influence of trace gas–aerosol interactions on the regional and global distributions of trace gases and aerosols. In the first part of this study [*Pozzoli et al.*, 2008], the aerosol-chemistry-climate model (ECHAM5-HAMMOZ) was described and compared to observations from the Transport and Chemical Evolution over the Pacific (TRACE-P) aircraft campaign in the Asian continental outflow (spring 2001). We also discussed the global and regional impacts of the trace gas–aerosol interactions on trace gas distributions. In this second part, we use the model to quantify the influence of trace gas–aerosol interactions on the global distributions and optical properties of aerosols. ECHAM5-HAMMOZ is particularly well suited for such a study as it includes a prognostic representation of size distribution and mixing state of the aerosol components (including sulfate, black carbon, organic carbon, sea salt and mineral dust), and is fully coupled with a comprehensive

Table 2. Heterogeneous Reactions and Uptake Coefficients Used in This Work

Reactions	Aerosol	Uptake Coefficients γ	References
$N_2O_5 \rightarrow 2HNO_3$	sulfate	$\gamma_{N_2O_5}$[a]	*Kane et al.* [2001], *Hallquist et al.* [2003]
$N_2O_5 \rightarrow 2HNO_3$	organic carbon	0.03(RH $\geq$ 50%); $5.2 \times 10^{-4} \times$ RH(RH < 50%)	*Thornton et al.* [2003]
$N_2O_5 \rightarrow 2HNO_3$	black carbon	0.005	*Sander et al.* [2003]
$N_2O_5 \rightarrow 2HNO_3$	sea salt	0.03 (RH $\geq$ 50%);0.005(RH < 50%)	*Atkinson et al.* [2004]
$N_2O_5 \rightarrow 2HNO_3$	mineral dust	0.003–0.02(30% $\leq$ RH $\leq$ 70%)	*Bauer et al.* [2004]
$NO_3 \rightarrow HNO_3$	wet aerosols[b]	0.001	*Jacob* [2000]
$NO_2 \rightarrow 0.5HNO_3 + 0.5HNO_2$	wet aerosols[b]	0.0001	*Jacob* [2000]
$HO_2 \rightarrow 0.5H_2O_2$	wet aerosols[b]	0.2	*Jacob* [2000]
$SO_2 \rightarrow SO_4^{2-}$ (aer)	sea salt	0.05(RH $\geq$ 50%);0.005(RH < 50)	*Song and Carmichael* [2001]
$SO_2 \rightarrow SO_4^{2-}$ (aer)	mineral dust	10^{-4}	*Ullerstam et al.* [2002, 2003]
$HNO_3 \rightarrow NO_3^-$ (aer)	mineral dust	0.1	*Bauer et al.* [2004]
$NO_3 \rightarrow NO_3^-$ (aer)	mineral dust	0.1	*Bian and Zender* [2003]
$O_3 \rightarrow$ products	mineral dust	10^{-5}	*Bauer et al.* [2004]

[a]$\gamma_{N_2O_5} = 10^{\beta(T)} \times (2.79 \times 10^{-4} + 1.3 \times 10^{-4} \times RH - 3.43 \times 10^{-6} \times RH^2 + 7.52 \times 10^{-8} \times RH^3)$; $\beta(T) = -4 \times 10^{-2} \times (T - 294)$ for T $\geq$ 282K; $\beta(T) =$ 0.48 for T < 282 K.

[b]Wet particles are defined as all the particles in the hydrophilic/soluble modes of HAM (NS, KS, AS and CS).

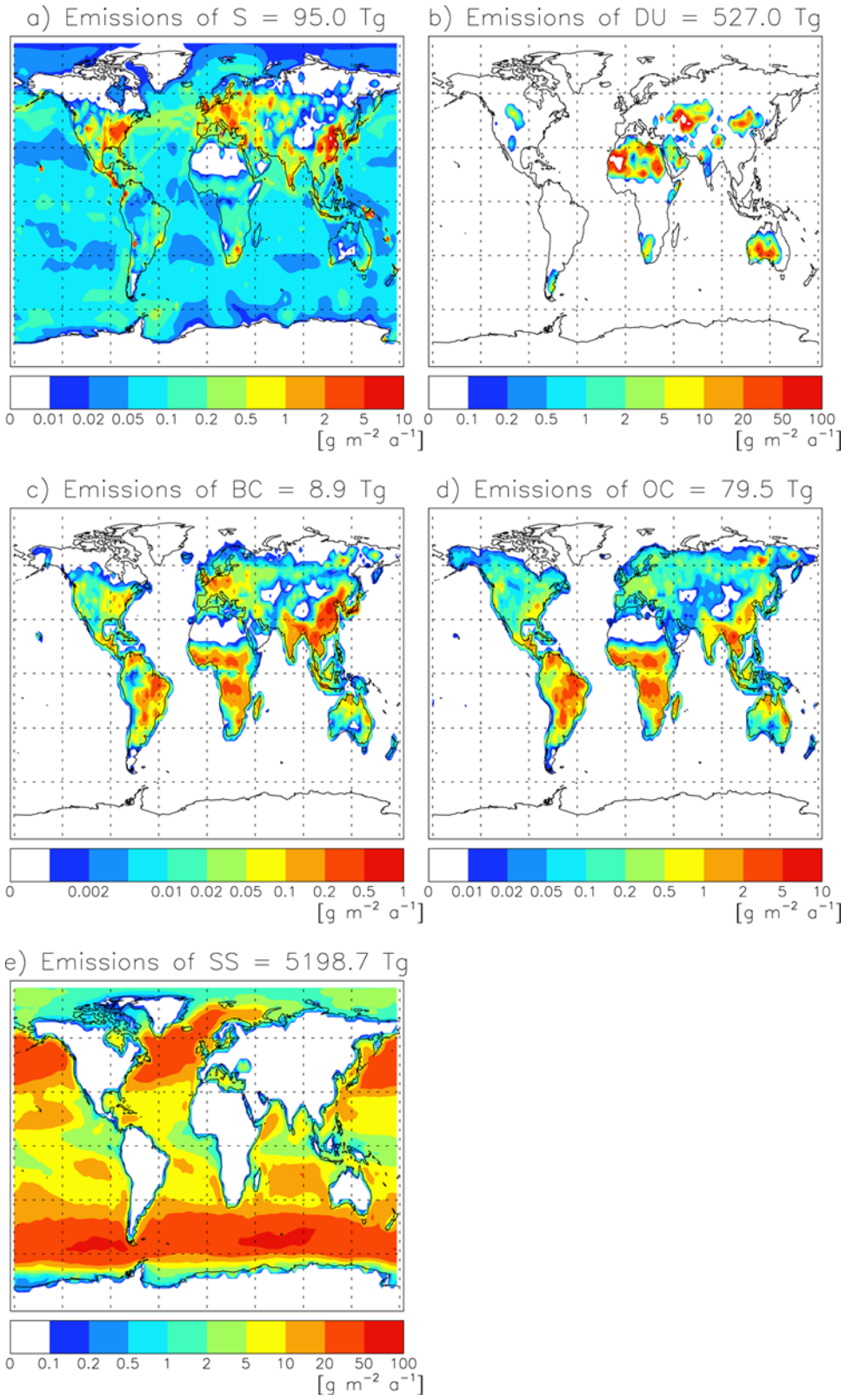

Figure 1. Annual emissions (g m^{-2} a^{-1}) of (a) total sulfur (S), (b) mineral dust (DU), (c) black carbon (BC), (d) organic carbon (OC), and (e) sea salt (SS).

trace gas simulation that includes sulfur and heterogeneous chemistry.

[5] In this work, after a short description of the model (section 2), we present the results of a series of sensitivity simulations which examine the impact of heterogeneous chemistry on aerosol distributions with a special focus on the reactions that follow SO_2 uptake on mineral dust and sea salt (section 3). Sections 4 and 5 provide a discussion

Table 3. Reactions and Processes Used in Each Sensitivity Simulation[a]

Labels	N_2O_5 on Wet Aerosols	NO_3 on Wet Aerosols	NO_2 on Wet Aerosols	HO_2 on Wet Aerosols	SO_2 on Sea Salt	SO_2 on Mineral Dust	HNO_3 on Mineral Dust	NO_3 on Mineral Dust	O_3 on Mineral Dust	Sulfate Formation on Sea Salt	Sulfate Formation on Dust	Mineral Dust Coating by SO_2 Uptake
BASE	yes	yes	yes	yes	yes	yes	yes	yes	yes	yes	yes	yes
NOHET												
NOHETDU	yes	yes	yes	yes	yes					yes		
NOSO4HET	yes	yes	yes	yes	yes	yes	yes	yes	yes			
NOCOAT	yes	yes	yes	yes	yes	yes	yes	yes	yes	yes	yes	

[a]"Yes" means that reactions and processes were included in the specific simulation.

of the main results and a summary with conclusions, respectively.

2. Model and Simulation Overview

2.1. Description of the ECHAM5-HAMMOZ Model

[6] The aerosol-chemistry-climate model ECHAM5-HAMMOZ [*Pozzoli et al.*, 2008; *Pozzoli*, 2007] is composed of the tropospheric chemistry module MOZECH (J. Rast et al., Sensitivity of a chemistry climate model to changes in emissions and the driving meteorology, manuscript in preparation, 2008) and the aerosol module HAM [*Stier et al.*, 2005]. The two modules are fully interactive and implemented together in the well established ECHAM5 general circulation model (GCM) [*Roeckner et al.*, 2003].

[7] ECHAM5 was developed at the Max Planck Institute for Meteorology on the basis of the numerical weather prediction model of the European Center for Medium-Range Weather Forecast (ECMWF) [*Simmons et al.*, 1989]. The prognostic variables of the model are vorticity, divergence, temperature and surface pressure. The multidimensional flux-form semi-Lagarangian transport scheme from *Lin and Rood* [1996] on a gaussian grid is used for water vapor and cloud variables and for the advection of chemical tracers. Stratiform clouds, cloud cover and cumulus convection are described by *Lohmann and Roeckner* [1996], *Tompkins* [2002], *Tiedtke* [1989], and *Nordeng* [1994]. In the current study, the radiative transfer calculation considers climatological vertical profiles of the main greenhouse gases (CO_2, O_3, CH_4, etc.) and cloud water and ice. The shortwave radiative transfer follows *Fouquart and Bonnel* [1980] considering 4 spectral bands, 1 for the visible-UV range (0.25–0.69 μm) and 3 for the IR (0.69–4 μm). The longwave radiative transfer scheme follows *Mlawer et al.* [1997] and *Morcrette et al.* [1998] and considers 16 spectral bands from 10 cm^{-1} to 3000 cm^{-1}.

[8] The tropospheric aerosol module HAM [*Stier et al.*, 2005] predicts the size distribution and composition of internally and externally mixed aerosol populations. The particle size distribution is described by 7 lognormal modes. Four modes are considered as hydrophilic internally mixed aerosols. Three additional modes are considered as hydrophobic aerosols composed of an internal mixture of black and organic carbon in the Aitken mode (KI), and of mineral dust in the accumulation (AI) and coarse (CI) modes (Table 1). The microphysical core of HAM, M7 [*Vignati et al.*, 2004], treats the aerosol dynamics and thermodynamics in the framework of the modal structure as described above. Dry deposition velocities are calculated with a serial resistance approach based on *Ganzeveld and Lelieveld* [1995] and *Ganzeveld et al.* [1998, 2006]. Wet deposition is differentiated between scavenging in stratiform and convective clouds, liquid and mixed clouds. Mode-specific scavenging parameters are used, with lower values for hydrophobic (externally mixed) modes [see *Stier et al.*, 2005, Table 3]. Aerosol optical properties (single scattering albedo, extinction coefficient and asymmetry factor) are precalculated explicitly from the Mie theory following *Toon and Ackerman* [1981] for a wide range of aerosol size distributions and refractive indices for 24 solar spectral bands and archived in a look-up table.

[9] The gas phase chemical scheme is identical to the one used in MOZART version 2 [*Horowitz et al.*, 2003] with small modification as described by *Pozzoli et al.* [2008]; in particular, the sulfur chemistry [*Feichter et al.*, 1996] is now included in the gas phase chemical mechanism. The photolysis rates are calculated online with the Fast-J.2 algorithm [*Bian and Prather*, 2002] which takes into account the simulated aerosol and cloud optical properties. The major heterogeneous reactions are included and the heterogeneous reaction rates explicitly account for the mixing states of aerosols (see Table 2 and *Pozzoli et al.* [2008, section 2.4] for details). We only describe here the heterogeneous reactions of SO_2 on sea salt and dust as they are especially important for this study.

[10] The SO_2 molecules adsorbed on the surface of sea salt particles are mainly oxidized by O_3 [*Chameides and Stelson*,

Table 4a. Global Annual Mean Burden, Sources, Lifetime, and Sinks (Wet Deposition, Dry Deposition, and Sedimentation) Simulated by ECHAM5-HAMMOZ (BASE Simulation)[a]

Species	Total Sources, Tg a^{-1}	Burden, Tg	Lifetime, days	Wet, %	Dry, %	Sedimentation, %
SO_4^{2-}	78.0	0.87	4.0	93.7	2.8	3.5
BC	8.9	0.13	5.3	92.2	7.6	0.3
OC	79.5	1.14	5.2	92.5	7.2	0.2
SS	5198.7	9.73	0.7	53.2	20.2	26.6
DU	527.0	5.65	3.8	58.4	5.5	36.1
SO_2	72.5	0.77	3.8			

[a]Mass units of sulfuric species are in Tg(S).

Table 4b. Sources of Sulfate[a]

Sulfate Sources	ECHAM5-HAMMOZ, Tg a^{-1}
Primary emissions	1.86 (2%)
SO_2 in-cloud oxidation	44.90 (57%)
SO_2 on sea salt	3.69 (5%)
SO_2 on dust	0.55 (<1%)
Condensation H_2SO_4	26.93 (34%)
Nucleation H_2SO_4	0.07 ($\ll$1%)
Total	78.00

[a]Mass units of sulfuric species are in Tg(S).

1992]. For this reaction we apply pH-dependent constant rate used for the SO_2 in-cloud oxidation by O_3 [*Maahs*, 1983]. Following *Alexander et al.* [2005], we assume that the alkalinity of sea salt particles is rapidly titrated by SO_2. Thus we only consider sulfate formation on fresh sea salt particles by oxidation with O_3 at a constant pH = 8 (fresh sea salt particles are diagnosed as the particles being only composed of sea salt and water). We do not take into account the sea salt alkalinity titration by HNO_3 (which can be important in tropical regions where NOx emissions dominate over SO_2 emissions [*Alexander et al.*, 2005]). We assume that the SO_2 uptake on aerosol is reversible [*Ullerstam et al.*, 2002], meaning that the fraction of SO_2 adsorbed on sea salt particles that does not form sulfate goes back into the gas phase, while the sulfate formed is added to the mass of the relevant aerosol mode.

[11] Following the recommendations of recent experimental studies [*Usher et al.*, 2002; *Ullerstam et al.*, 2002] and previous modeling works [*Bauer and Koch*, 2005; *Liao and Seinfeld*, 2005], we use a "reactive" uptake coefficient of 10^{-4} for SO_2 on mineral dust and assume that all the SO_2 molecules adsorbed on dust particles produce sulfate. It should be noted that the uptake coefficient of SO_2 on mineral dust is highly uncertain. For example, *Liao et al.* [2004] and *Liao and Seinfeld* [2005] used the uptake coefficient proposed by *Dentener et al.* [1996] (0.1 for RH $\geq$ 50% and 10^{-3} for RH < 50%), while *Bauer and Koch* [2005] used a much smaller value for the SO_2 uptake

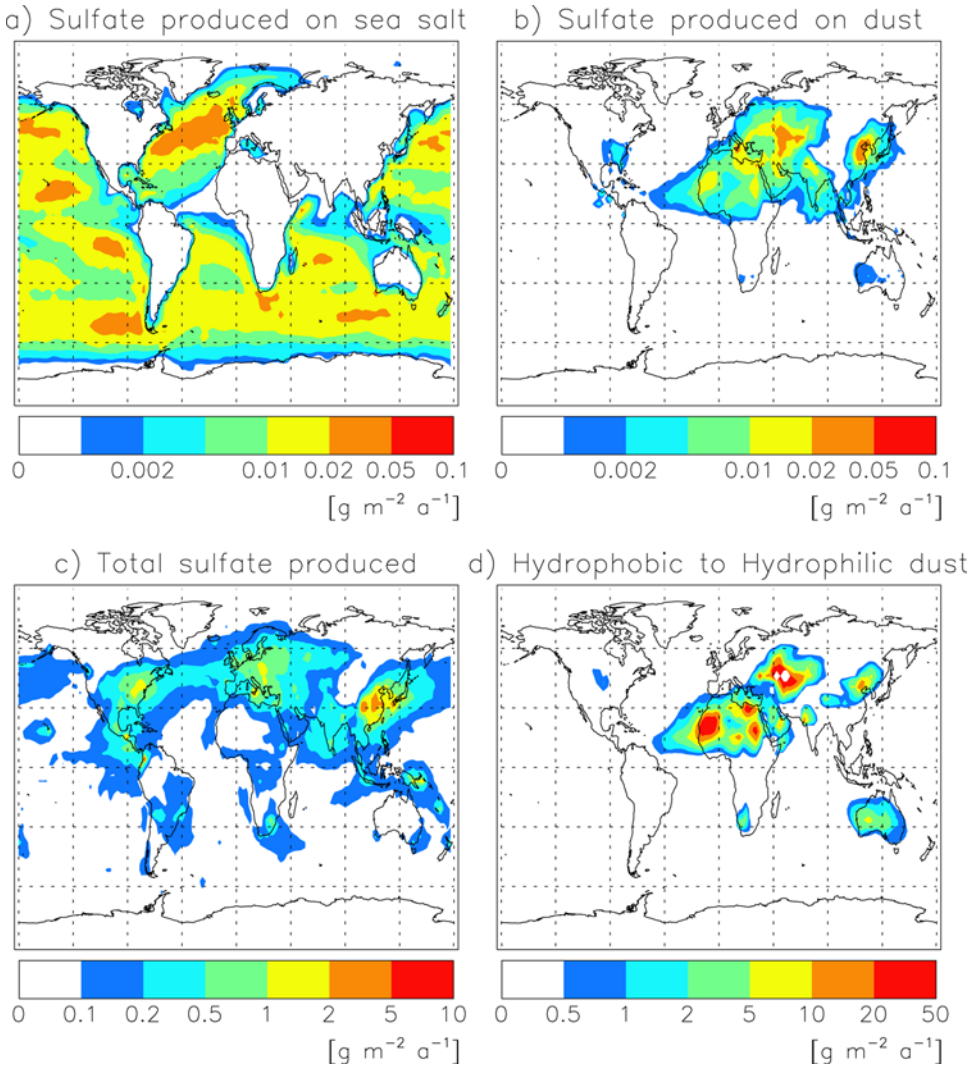

Figure 2. Sulfate (g(S) m^{-2} a^{-1}) formed on (a) sea salt and (b) mineral dust particles, (c) total sulfate production, and (d) the mass of mineral dust (g m^{-2} a^{-1}) that is transferred from an hydrophobic to a hydrophilic mode because of sulfate coating of the dust particle surface.

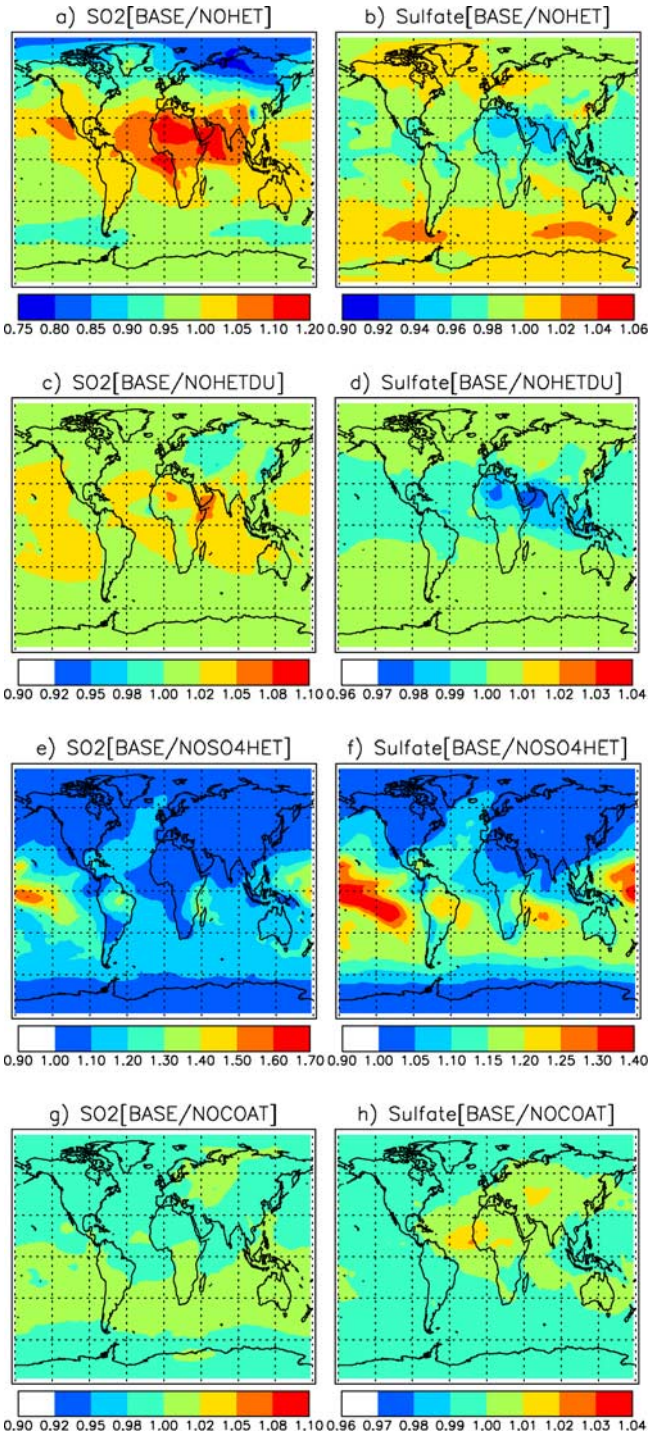

Figure 3. Ratio of SO_2 and sulfate annual mean total burdens between BASE simulation and the sensitivity simulations (a and b) NOHET, (c and d) NOHETDU, (e and f) NOSO4HET, and (g and h) NOCOAT.

coefficient on dust (10^{-4} for RH > 60% and 10^{-7} for dryer conditions following the experimental work of *Ullerstam et al.* [2002] and *Usher et al.* [2002, 2003]). Another source of uncertainty is the alkalinity of the dust particles which may influence the heterogeneous reactions of SO_2 and HNO_3. *Liao et al.* [2003], for example, assumed that these reactions occur only if the dust alkalinity exceeds the acidity from the dust-associated sulfate and nitrate. In our current model version the alkalinity of dust particles is not taken into account. We account for the saturation of the dust particles and consider a particle to be saturated when it is covered by a monolayer of sulfate molecules. Thus externally mixed insoluble dust particles may become soluble because of sulfate coating by SO_2 uptake and be transferred to the corresponding soluble modes.

[12] We used the RETRO project data set of year 2000 (http://www.retro.enes.org/) for the surface CO, NOx and hydrocarbons anthropogenic emissions (T. Pulles et al., The application of the emission inventory model team: Global emissions from fuel combustion in the years 1960 to 2000, submitted to *Atmospheric Environment*, 2007; M. Schultz et al., A global data set of anthropogenic CO, NOx, and NMVOC emissions for 1960–2000, manuscript in preparation, 2008) and wildfire emissions [*Schultz et al.*, 2008]. A climatology of typical injection vertical profiles is used for forest and savannah fire emissions (D. Lavoué, personal communication, 2005). Aircraft NO emissions are from *Grewe et al.* [2002]. Lightning NOx emissions are parameterized following *Grewe et al.* [2001], and are proportional to the calculated flash frequency and distributed vertically using a C-shaped profiles. Lightning frequency is brought to a value that results in 3 TgN a^{-1} (Rast et al., manuscript in preparation, 2008). The biogenic VOC emissions are calculated online with the MEGAN module of *Guenther et al.* [1995]. The anthropogenic and fire aerosol emissions are based on the AEROCOM emission inventory [*Dentener et al.*, 2006] representative of the year 2000. SO_2 emissions include volcanoes [*Andres and Kasgnoc*, 1998; *Halmer et al.*, 2002], vegetation fires [*van der Werf et al.*, 2003], industry, fossil fuel and biofuel [*Cofala et al.*, 2005]. Except DMS, 97.5% of all sulfuric emissions are in the form of SO_2 and 2.5% in the form of primary sulfate particles. The emissions of dust and sea salt are wind driven following *Tegen et al.* [2002] and *Schulz et al.* [2004], respectively. Marine DMS emissions are based on DMS seawater concentrations of *Kettle and Andreae* [2000] and the air-sea exchange rate from *Nightingale et al.* [2000]. Terrestrial biogenic DMS emissions follow *Pham et al.* [1995]. The annual mean emission for sulfur is 95 Tg(S) a^{-1}, 527 Tg a^{-1} for mineral dust, 8.9 Tg a^{-1} for black carbon, 79.5 Tg a^{-1} for organic carbon and 5199 Tg a^{-1} for sea salt (Figure 1).

2.2. Simulation Setup

[13] For the present study we used ECHAM5-HAMMOZ with a spectral resolution of T42 corresponding to about 2.8 × 2.8 degrees in the horizontal dimension and 31 vertical levels from the surface up to 10 hPa, and with a 20-min time step. In order to reproduce consistent meteorological conditions for the year 2001, the model was driven by the ECMWF ERA40 meteorological fields. In that configuration, the prognostic variables of ECHAM5 (vorticity, divergence, temperature and surface pressure) are relaxed toward the ERA40 reanalysis data every 3 h [*Jeuken et al.*, 1996]. Five simulations were conducted for 2001 (Table 3): (1) In the BASE simulation, all the couplings between the chemistry and aerosol modules are included, i.e., including sulfur chemistry, heterogeneous reactions (including all reactions listed in Table 2) and effect of

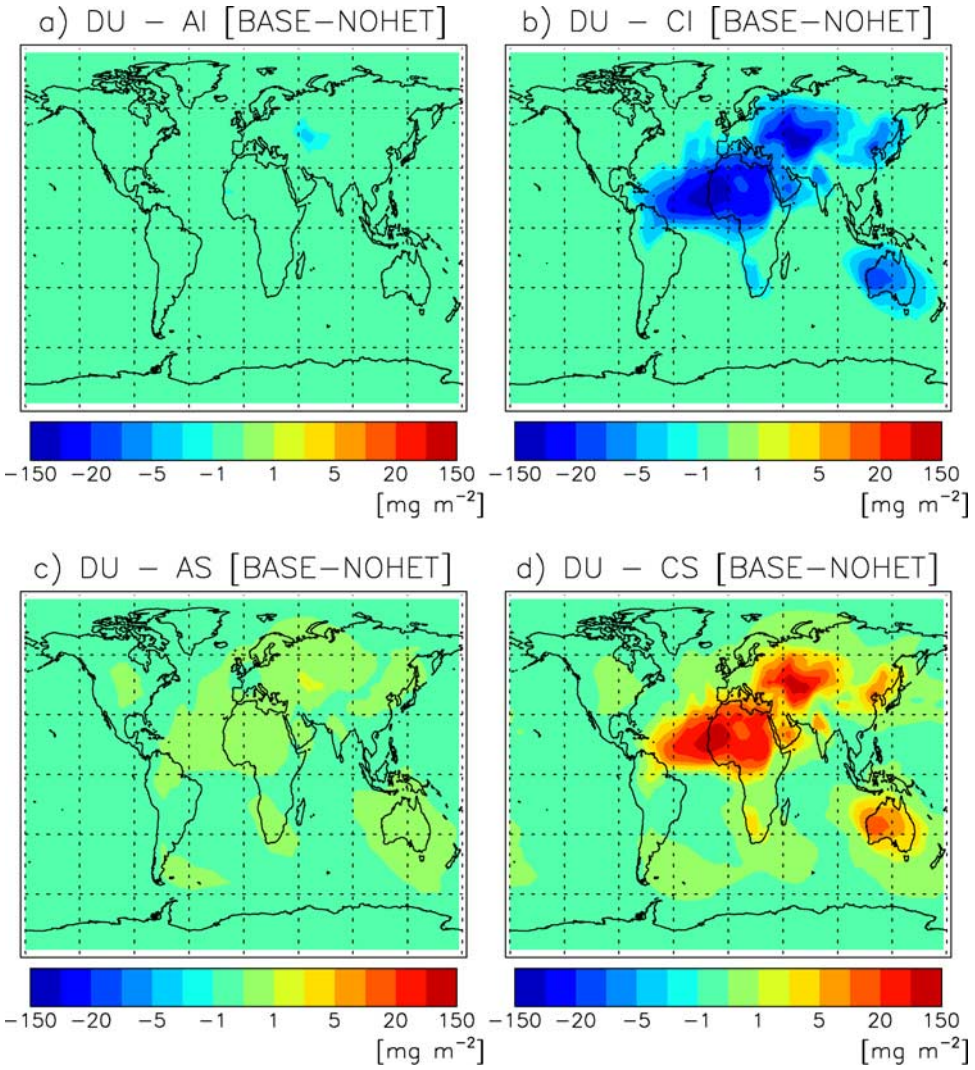

Figure 4. Annual mean burdens differences (mg/m^2) between BASE and NOHET simulations of mineral dust in the (a) accumulation (DU-AI) and (b) coarse hydrophobic (DU-CI) modes and in the (c) accumulation (DU-AS) and (d) coarse (DU-CS) hydrophilic modes.

aerosols on photolysis reaction rates. (2) The NOHET simulation is the same as BASE but no heterogeneous chemistry is accounted for. (3) The NOHETDU simulation is the same as BASE but no heterogeneous chemistry on mineral dust is accounted for. (4) The NOSO4HET simulation is the same as BASE but no sulfate aerosol production from SO_2 uptake on sea salt and dust is accounted for. (5) The NOCOAT simulation is the same as BASE but no coating of dust after SO_2 uptake is accounted for. These sensitivity simulations were intended to asses the impacts of the whole set of heterogeneous reactions implemented in the model (NOHET), of the heterogeneous reactions on mineral dust (NOHETDU), of the sulfate produced by reactive uptake of SO_2 on dust and sea salt (NOSO4HET), and of the effect of ageing of dust particles by sulfate coating (NOCOAT) on the aerosol distributions, concentrations and optical properties. We conducted a 1-year spin-up (from January to December 2000) for the BASE simulation and a 1-month spin-up starting in December 2000 for the sensitivity simulations. In this study the aerosol optical properties calculated by HAM were used only as diagnostics; that is, they did not feedback on the ECHAM5 radiative transfer scheme which insures identical meteorology in the different sensitivity simulations.

3. Influence of Trace Gas–Aerosol Interactions on Sulfur Species and Aerosols

[14] In the following we quantify the impact of heterogeneous reactions on the distribution of SO_2, sulfate, dust and black carbon. The simulated aerosol distributions and budget are briefly described and evaluated in the auxiliary material.[1] Simulated aerosol concentrations are evaluated using measurements from the European Monitoring and Evaluation Program (EMEP) and from the North American Interagency Monitoring of Protected Visual Environments

[1]Auxiliary materials are available in the HTML. doi:10.1029/2007JD009008.

Table 5. Ratios Between Global Annual Mean Burdens of Total Black Carbon (BC) and Mineral Dust (DU) and for Hydrophobic (KI, AI, and CI) and Hydrophilic (KS, AS, and CS) Modes Calculated by the Sensitivity Simulations[a]

Species	BASE	BASE / NOHET	BASE / NOHETDU	BASE / NOSO4HET	BASE / NOCOAT
BC KI	2.20×10^{-2}	1.04	1.01	0.93	1.00
BC KS	5.85×10^{-3}	1.03	1.01	0.96	1.00
BC AS	1.04×10^{-1}	1.00	1.00	1.01	1.00
BC CS	2.03×10^{-4}	1.28	1.20	1.09	1.15
BC TOT	0.13	1.00	1.00	0.99	1.00
DU AI	0.02	0.57	0.55	0.49	0.50
DU CI	1.46	0.49	0.48	0.44	0.44
DU AS	0.08	1.15	1.17	1.24	1.24
DU CS	4.09	1.45	1.47	1.60	1.59
DU TOT	5.65	0.95	0.95	0.94	0.94

[a]Unit is Tg.

(IMPROVE) networks and simulated aerosol optical depth are compared to measurements from the Aerosol Robotic Network (AERONET). The evaluation of the model can be summarized as follows. The simulated sulfate concentrations are in general in good agreement with the observations from EMEP (Figures S3 and S4 in the auxiliary material) and IMPROVE (Figures S5 and S6 in the auxiliary material) networks, while the SO_2 concentrations are largely overestimated over Europe (Figures S3 and S4 in the auxiliary material). The model reproduces fairly well the AOD seasonal variations in most of the considered AERONET stations (Figure S7 and Table S1 in the auxiliary material). We find a burden of 0.77 and of 0.87 Tg(S) a^{-1} for SO_2 and sulfate (Tables 4a and 4b), respectively.

3.1. SO_2 and Sulfate

[15] SO_2 and sulfate play an important role both in the formation of aerosol particles and in the ageing processes of existing particles. They also impact strongly the aerosol composition, mixing state, and therefore the number and size distribution, optical properties, and lifetime of other aerosols. In ECHAM5-HAMMOZ, sulfate aerosol sources are primary emissions, nucleation (formation of new fine particles), condensation of H_2SO_4 on all aerosol modes, in-cloud oxidation of SO_2, and heterogenous reaction of SO_2 on sea salt and mineral dust particles. The production of sulfate by nucleation is not very important in terms of mass (global annual sulfate production = 0.07 Tg(S), Table 4a and 4b), but is important in terms of number of particles. In the BASE simulation the nucleation mode contributes 96% to the total particle number concentration in the troposphere (not shown). Condensation of H_2SO_4 with formation of sulfate on the surface of existing particles is important in terms of sulfate mass with 27 Tg(S) produced per year and also because it is responsible for the ageing of hydrophobic particles (black carbon and organic carbon in the Aitken mode and mineral dust in the accumulation and coarse modes). In-cloud oxidation of SO_2 is the most significant process that leads to sulfate production with 45 Tg(S) produced per year. The sulfate aerosol formed by this later process is distributed to the accumulation and coarse mode aerosol particles according to their number concentrations.

[16] Heterogeneous reactions influence these processes through the direct uptake of SO_2 on sea salt and mineral dust particles. Figure 2 shows the sulfate production rates by uptake of SO_2 on sea salt (Figure 2a) and mineral dust (Figure 2b). The sulfate formation on dust and sea salt accounts for 0.55 Tg(S) a^{-1} (<1%) and 3.69 Tg(S) a^{-1} (5%), respectively (Tables 4a and 4b). The sulfate formation on dust has only little significance in terms of total sulfate production (Figure 2c), but has important implications for mineral dust as hydrophobic particles are transformed into hydrophilic particles following surface coating by sulfate (Figure 2d). 300 Tg a^{-1} of dust are transferred from a hydrophobic-insoluble modes (AI and CI) to the corresponding hydrophilic-soluble modes (AS and CS), which represent more than half of the insoluble mineral dust particles emitted (527 Tg a^{-1}, Figure 1b).

3.1.1. Impact of Heterogeneous Reactions on SO_2

[17] The impact of the overall set of heterogeneous reactions (Table 2) is quantified by comparing the BASE and NOHET simulations. Figure 3a shows that the SO_2 burden increases by 5–10% over a large area in the Northern Hemisphere and by more than 10% over the Sahara, the Gulf of Guinea, and the Arabian Peninsula but decreases in the Southern Hemisphere by up to 10% (except over the continents). The SO_2 burden also decreases north of about 40°N, up to 20% at high latitudes (14% decrease in terms of annual mean surface concentration). These results reflect in fact the impacts of competing processes. The SO_2 uptake on sea salt and dust induces a decrease of SO_2. In the mean time, the overall set of heterogeneous reactions (Table 2) and in particular the O_3 uptake on dust and the N_2O_5 and HO_2 reactions on wet particles induce a global reduction of O_3 and OH by 9% and 10%, respectively [*Pozzoli et al.*, 2008]. This, in turn, affects the SO_2 and DMS distributions. The SO_2 and DMS oxidation by OH decreases, leading to a decrease in H_2SO_4 production, and in the associated sulfate production by condensation on existing particles, while a higher SO_2 concentration may increase sulfate production by SO_2 in-cloud oxidation.

3.1.2. Impact of Heterogeneous Reactions on Sulfate

[18] Figure 3b illustrates the overall impact of the full set of heterogeneous reactions on sulfate burden. The competing effects previously described result in a 1% increase in the global annual SO_2 burden and in a 2% decrease in global annual mean sulfate burden. Sulfate burden increases by +4% over the oceans in the Southern Hemisphere, and decreases in the tropics with a maximum between 4 and 6% over the Sahara Desert, Arabian Peninsula, and India. Whereas heterogeneous chemistry is found to cause a large decrease in SO_2 at high latitudes in the Northern Hemisphere, it leads only to a small increase in sulfate (2% in terms of global burden and 3% in terms of annual mean surface concentration). Figure 3f compares the BASE simulation and the NOSO4HET simulation in which the heterogeneous uptake of SO_2 is only considered as a sink for this species. The heterogeneous reactions of SO_2 on aerosols increase the sulfate burden over the oceans (by up to 30% and 40% over the Pacific ocean). The sulfate formation on sea salt and mineral dust increases globally the sulfate burdens by 10% (BASE/NOSO4HET). These changes are most likely due to sea salt uptake, because the sulfate produced on dust is small compared to other sulfate sources (only 0.55 Tg(S) a^{-1}, Table 4a and 4b), and also because we do not find changes in sulfate and SO_2 burdens when we

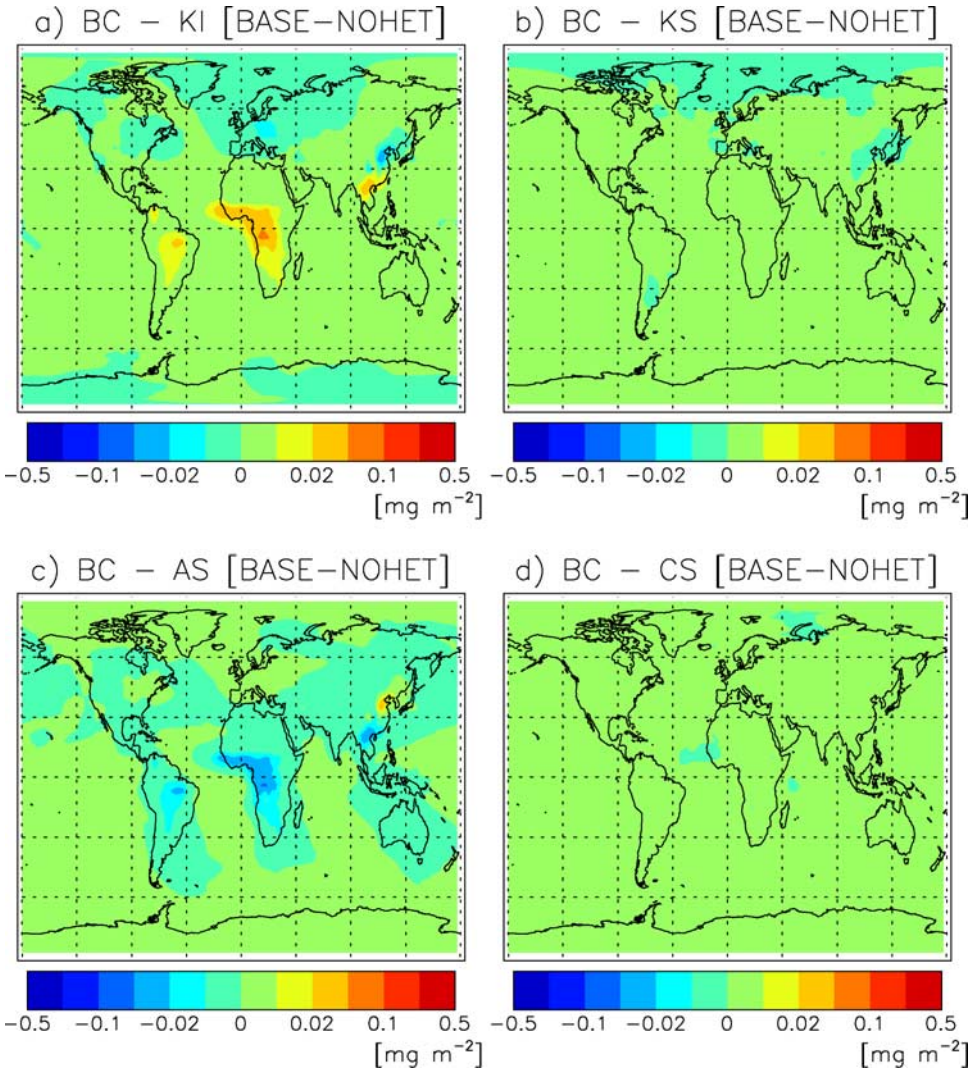

Figure 5. Annual mean burdens differences (mg/m^2) between BASE and NOHET simulations of black carbon in the (a) Aitken hydrophobic (BC-KI) mode and in the (b) Aitken (BC-KS), (c) accumulation (BC-AS), and (d) coarse (BC-CS) hydrophilic modes.

exclude the coating of externally mixed particles (Figure 3h, BASE/NOCOAT).

3.2. Mineral Dust and Black Carbon

[19] The heterogeneous reactions included in our study influence the distributions of other aerosol species either directly (e.g., mineral dust can be coated by sulfate from SO_2 uptake) or indirectly (e.g., by changing the SO_2 oxidation rate which determines the H_2SO_4 concentration and therefore its condensation on existing particles).

3.2.1. Impact of Heterogeneous Reactions on Dust

[20] Figure 4 shows the change in dust aerosol mass due to the inclusion of the whole set of heterogeneous reactions (BASE-NOHET), while Table 5 summarizes the annual mean global burden changes in mineral dust in the sensitivity simulations. As previously mentioned, we assume that mineral dust particles become hydrophilic once coated by a monolayer of sulfate molecules (section 2.1). The impact of this process is shown in Figure 4. More than 100 mg m^{-2} of dust (annual mean burden difference) is redistributed from the insoluble to the soluble coarse mode. The annual mean global burden of dust decreases by 5% because of all heterogeneous reactions (Table 5, BASE/NOHET) but the changes in the single modes are larger, −43% and −51% in the accumulation and coarse insoluble modes, respectively, and +15% and +45% in the accumulation and coarse soluble modes, respectively. The decrease of 5% in total burden is due to a higher wet deposition efficiency of soluble mineral dust particles. The NOSO4HET and NOCOAT simulations give similar results, i.e., an increase in the insoluble modes (AI and CI) and a decrease in the soluble modes (AS and CS) with respect to the BASE simulation. The differences between these two simulations and the BASE simulation provide an estimate of the significance of the sulfate formation and coating of dust for the transfer of dust particles from the insoluble to soluble modes. In the BASE simulation the insoluble dust (sum of the accumulation and coarse modes) accounts for 26% of the total burden of dust (Table 5), while in the

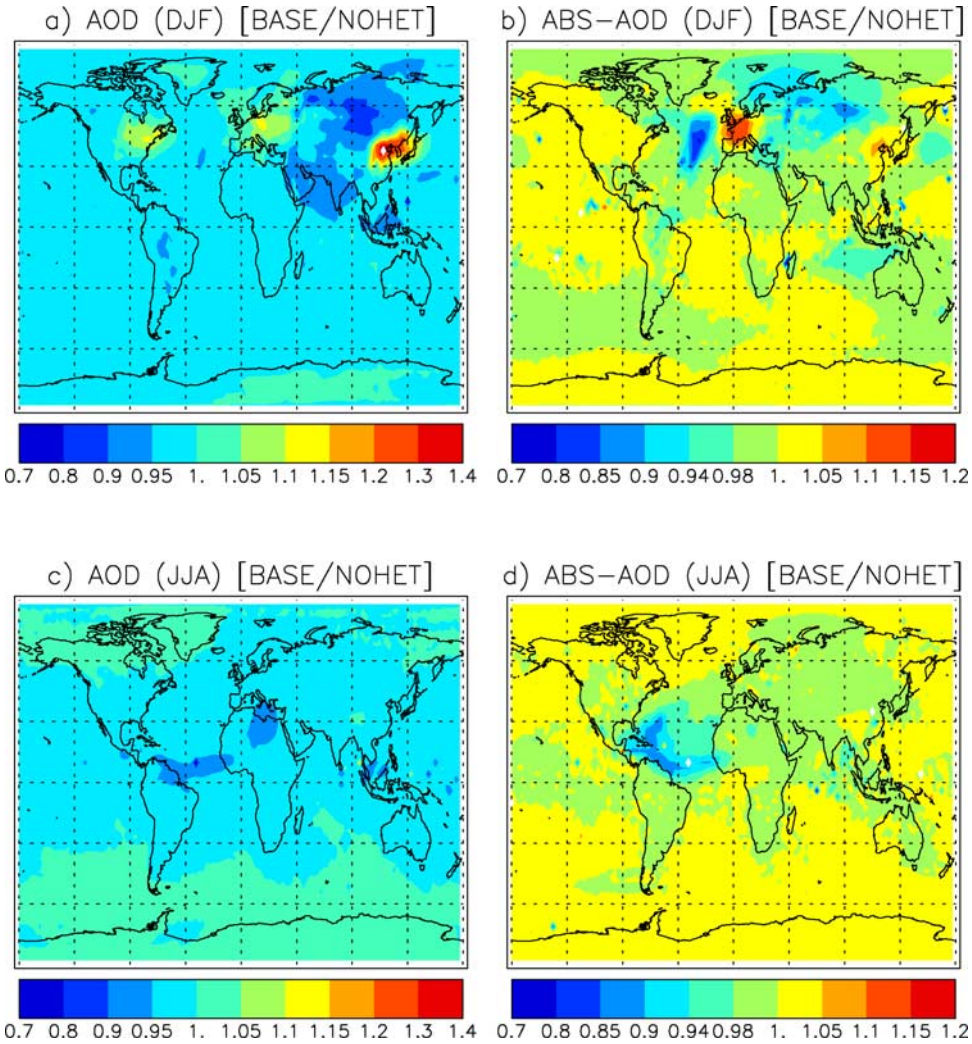

Figure 6. Ratio between BASE and NOHET simulations of seasonal mean (a) aerosol optical depth AOD and (b) absorption optical depth ABS in winter (DJF) and (c) aerosol optical depth AOD and (d) absorption optical depth ABS in summer (JJA).

NOCOAT simulation (in which the ageing of dust particles does not occur after SO_2 uptake) the insoluble fraction of dust is 56%.

3.2.2. Impact of Heterogeneous Reactions on Black Carbon

[21] The effect of heterogeneous reactions on the black carbon distribution is shown on Figure 5. Hydrophobic black carbon aerosol mass decreases in the Northern Hemisphere (Figure 5a), especially over polluted regions, eastern U.S., Europe, and China. By contrast, the black carbon burden increases in the insoluble Aitken mode (KI) over regions where biomass burning sources emit high loads of carbonaceous aerosols (central Africa, Amazonia and southeast Asia). This increase can be related to the decrease of oxidant concentrations due to heterogeneous reactions which results in less SO_2 oxidation and hence less H_2SO_4 condensation on hydrophobic particles (see section 3.1). This change in ageing is reflected in the accumulation soluble mode (AS) (Figure 5c), but the total global burden of black carbon does not change between the BASE and NOHET simulations as shown in Table 5. The effect of heterogeneous reactions on dust (BASE/NOHETDU) is not relevant for black carbon. The black carbon burden only increases in the soluble coarse mode by 20% but the burden in this particular mode is very low.

[22] We do find an indirect effect of the formation of sulfate on mineral dust and sea salt on black carbon (Table 5, BASE/NOSO4HET). When we do not consider this additional sulfate formation, we find a black carbon burden decrease of 7% and 4% in the Aitken insoluble and soluble modes, respectively. As we do not find any additional effect on black carbon due to the coating of insoluble mineral dust particles (BASE/NOCOAT), we suggest that the increase in black carbon in the coarse soluble mode in the BASE simulation is probably due to an increase in coagulation efficiency as more wet particles are available.

3.3. Aerosol Optical Properties

[23] The trace gas−aerosol interactions and their subsequent effect on the aerosol distributions affect the optical properties of the particles. *Stier et al.* [2006] explored to what extent non absorbing aerosol species, like sulfate,

Table 6. Ratios Between Global Annual Means of Total Aerosol Optical Depth (AOD) and Total Absorption Optical Depth (ABS) and for Hydrophobic (KI, AI, an CI) and Hydrophilic (KS, AS, and CS) Modes Calculated by the Sensitivity Simulations

Species	BASE	$\frac{BASE}{NOHET}$	$\frac{BASE}{NOHETDU}$	$\frac{BASE}{NOSO4HET}$	$\frac{BASE}{NOCOAT}$
Total AOD	1.31×10^{-1}	0.98	0.99	1.03	1.00
AOD of KS	5.16×10^{-4}	0.98	0.98	1.03	0.89
AOD of KI	6.45×10^{-4}	1.04	1.01	0.93	1.42
AOD of AS	6.23×10^{-2}	0.97	0.99	1.08	1.00
AOD of AI	1.31×10^{-4}	0.57	0.55	0.49	0.50
AOD of CS	6.58×10^{-2}	1.02	1.02	1.03	1.03
AOD of CI	1.60×10^{-3}	0.47	0.47	0.42	0.43
Total ABS	2.16×10^{-3}	1.00	0.99	0.99	0.99
ABS of KS	5.37×10^{-5}	1.03	1.00	0.96	0.97
ABS of KI	2.47×10^{-4}	1.04	1.01	0.93	1.00
ABS of AS	1.67×10^{-3}	0.99	1.00	1.01	1.00
ABS of AI	9.42×10^{-7}	0.57	0.55	0.49	0.50
ABS of CS	1.39×10^{-4}	1.44	1.45	1.58	1.58
ABS of CI	4.86×10^{-5}	0.49	0.48	0.44	0.44

affect atmospheric absorption and the amount of diffuse solar radiation. For example atmospheric absorption can be reduced by the ageing of black carbon insoluble particles (enhancing their removal by wet scavenging), and increased by internal mixing (internal mixing of black carbon with non absorbing aerosols increases the absorption efficiency of black carbon [*Ackerman and Toon*, 1981]) and by increased diffuse solar radiation. *Stier et al.* [2006] found for example that SO_2 anthropogenic emissions increase aerosol absorption by 20–30% near the source regions. In this section we will similarly quantify the effect of heterogeneous reactions on these processes.

[24] On an annual mean basis the change in AOD when heterogeneous reactions are included are in the range of ±5% (not shown), but larger differences are seen regionally and seasonally. Figure 6a shows that in winter heterogeneous chemistry increases aerosol optical depths over the most polluted regions, e.g., by 5 to 15% over Europe and the eastern U.S. and by more than 30% over east Asia. This is explained by the increase in sulfate burden in the same region and season (up to 10% over east Europe and east U.S., up to 50% over east Asia, not shown). The aerosol absorption optical depth (ABS, defined by the product of the aerosol optical depth and the aerosol co-single-scattering albedo) in winter also increases by 5–10% in these regions with the largest enhancement (up to 15%) occurring over western Europe (Figure 6b).

[25] By contrast, we find a decrease of 20% in aerosol ABS over the north Atlantic Ocean and from 5 to 15% over Scandinavia and Siberia. The total black carbon burden (sum of the BC burdens over all the aerosol modes) remains more or less constant (changes, in general, are between ±4%) but the changes in the mixing state of black carbon particles can be important in determining aerosol absorption. We find that the inclusion of heterogeneous chemistry significantly changes ABS only on a regional and seasonal basis. In winter, for example, where the largest differences are seen, we find a colocation of the increase in ABS (Figure 6b) and the increase in the black carbon burden in the accumulation soluble mode (Figure 5c) over Europe, U.S., and northern China (Beijing and Yellow Sea). *Stier et al.* [2006] found that the ABS increases over sulfate source regions because of the internal mixing while it decreases over remote regions (North Atlantic Ocean, Scandinavia and Siberia) because of enhanced black carbon wet deposition efficiency. Figure 6b provides further evidence for these two competing effects that contribute to atmospheric absorption.

[26] The global effects of heterogeneous reactions on annual mean aerosol optical properties are listed in Table 6 for all the particles and for each aerosol mode. The heterogeneous reactions on mineral dust play an important role as the two ratios BASE/NOHETDU and BASE/NOHET are very similar. We find a decrease in AOD in the accumulation and coarse insoluble modes of about 50% (the two modes being solely composed by mineral dust) because of SO_2 uptake, and small changes in the corresponding accumulation and coarse soluble modes, −3% and +2%, respectively. On the other hand, the AOD in these two soluble mode (AS and CS) is 10 times larger than that in the insoluble modes (AI and CI) (Table 6), so the overall AOD change is only ∼1% on the global annual mean. The sulfate formation on sea salt and mineral dust particles increases the annual global mean AOD by 3% (BASE/NOSO4HET). The AOD of the soluble modes increases (up to 8% in the accumulation mode), while the AOD of the insoluble modes decreases (in particular for the accumulation and coarse mode (>50%), but also for the Aitken mode (7%)). The sulfate formation from heterogeneous reactions and the coating of dust particles have also an indirect effect on insoluble particles in the Aitken mode (mixture of black carbon and organic carbon), the AOD in the Aitken mode decreases by 11% for soluble particles and increases by 42% for insoluble particles between the BASE and the NOCOAT simulations.

[27] The mode which contributes the most to the total ABS by aerosols is the accumulation soluble mode, followed by the Aitken insoluble and coarse soluble. The accumulation soluble mode does not change significantly in all the sensitivity simulations, which explains the small changes in the annual mean of total ABS. The Aitken insoluble mode (that is composed of an internal mixture of black and organic carbon) only changes by 4% because of the heterogeneous reactions (BASE/NOHET). The sulfate formation on sea salt and dust changes the ABS of this mode by −7% (BASE/NOSO4HET). The coating of dust particles by SO_2 uptake leads to a transfer from the insoluble to the soluble modes that results in a decrease of the ABS by 51% in the insoluble modes and to an increase of the ABS in the soluble modes by 58% while the total ABS decreases only by 1%. These changes are mainly due to the coating of the particles by sulfate formation from SO_2 uptake, as shown by the ratios BASE/NOSO4HET and BASE/NOCOAT.

4. Discussion

[28] We find annual mean burden of 0.77 and 0.87 Tg(S) for SO_2 and sulfate, respectively, in the BASE simulation. These numbers are within the range of those from other studies even though a comparison to EMEP observations indicate that our simulated SO_2 concentrations are over-

estimated by a factor of ~3.5 over Europe (section 2 of the auxiliary material). 57% of the total sulfate sources originates from SO_2 in-cloud oxidation by O_3 and H_2O_2, about 5% from heterogeneous reactions on sea salt and mineral dust particles, 34% from condensation on existing particles and nucleation of H_2SO_4 (produced again by SO_2 and DMS in the gas phase oxidation), the remaining 2% being primary emissions (Tables 4a and 4b).

[29] The value found for in-cloud oxidation of SO_2 by O_3 and H_2O_2 is very similar to the value of 41.3 Tg(S) a^{-1} found by *Liao et al.* [2003], but 2 times larger than that of *Bell et al.* [2005] (they do not consider aqueous oxidation by O_3 and pH of the clouds), and 2.5 times larger than that of *Alexander et al.* [2005] (they consider a constant cloud droplet pH of 4.5 that limits the impact of the O_3 relative to the H_2O_2 oxidation pathway).

[30] *Bauer and Koch* [2005] found a decrease of 30% (0.46 Tg(S)) in the global SO_2 burden because of the uptake of SO_2 on mineral dust and an increase of 4% in the total sulfate burden (0.50 Tg(S)), with 0.37 Tg(S) of sulfate present as externally mixed particles and the remaining sulfate associated to dust. These variations are larger than those found in this work (section 3.1), but the comparison between these two studies is difficult. Even if they used a SO_2 uptake coefficients of 10^{-4} (RH > 60%) and 10^{-7} (RH < 60%), which is close to the one used in the present work (10^{-4} for all RH conditions, Table 2), *Bauer and Koch* [2005] used different hypothesis for the coating of mineral dust particles, assuming that a dust particle is soluble when 10% of its surface is covered by sulfate.

[31] The studies of *Liao et al.* [2004] and *Liao and Seinfeld* [2005] are close to our study in terms of the uptake coefficients chosen for heterogeneous reactions (at least for the uptake of N_2O_5, HO_2, NO_2, and NO_3 on wet particles, of O_3 and HNO_3 on dust and of SO_2 on sea salt), but the description of aerosols is different (in their model aerosols are described with a bulk approach of external mixture of dust, organic carbon, black carbon and an internal mixture of inorganic aerosols like ammonium, sulfate, nitrate and sea salt). In comparison to our model, they used a higher SO_2 uptake coefficient on mineral dust (0.1 for RH > 50%, 3×10^{-4} for RH < 50%, from *Dentener et al.* [1996]), and the same SO_2 uptake coefficient on sea salt, but different assumptions on SO_2 uptake and sulfate formation. The work of *Liao et al.* [2004] suggests larger differences in sulfate and SO_2 burden due to heterogeneous reactions than our study (i.e., global mean sulfate and SO_2 burden decrease by 36% and 20%, respectively). *Liao et al.* [2004] found a sulfate burden of 0.6 Tg(S), including 0.06 Tg(S) (9%) associated with sea salt and 0.1 Tg(S) (16%) associated with dust. The total contribution of 25% due to heterogeneous formation of sulfate is larger than the 10% found in our work (section 3.1). The differences with *Liao et al.* [2004] may arise from the use of a different uptake coefficient of SO_2 on mineral dust and from different assumptions (e.g., they assumed that the pH of sea salt aerosols is always high enough to have an efficient SO_2 oxidation by O_3). On the other hand, we obtained a global annual sulfate production in sea salt particles by SO_2 uptake of 3.69 Tg(S) a^{-1}, which is very close to that found by *Alexander et al.* [2005], who constrained their model study with oxygen isotope measurements that can be used as an indication of SO_2 oxidation by O_3 in the aqueous phase. Similarly to *Alexander et al.* [2005], we assumed that the alkalinity is titrated by sulfate formation and therefore we allowed sulfate formation to occur only on "fresh" sea salt particles.

[32] We find that the model reproduces fairly well sulfate concentrations as discussed in section 2 of the auxiliary material and by *Pozzoli et al.* [2008] but overestimates SO_2 concentrations. This may indicate that more SO_2 molecules than what we assumed are adsorbed irreversibly on sea salt and dust particles independently on the effective sulfate formation, which further depends on SO_2 oxidation by O_3. The *Bauer and Koch* [2005] study indicates that the total sulfate aerosol mass changes by 20 to 40% and the externally mixed sulfate aerosol burden changes by up to 80% in response to a SO_2 uptake coefficient on dust ranging from 10^{-8} to 10^{-3}, which indicates that the overall budget is quite sensitive to that parameter. One limitation in our work arises from the large uncertainty associated with SO_2 uptake. In particular, for dust uptake of SO_2 we used a "reactive" uptake coefficient, which may account well for sulfate formation but not for the loss of SO_2 on dust particles. The effect of coating and surface saturation also need to be explored in detail by testing different ratios of sulfate amount needed to make a dust particle soluble as this leads to large differences in the mineral dust mixing state with possible feedbacks on other aerosol species.

5. Summary and Conclusions

[33] In this work we used the newly developed fully coupled aerosol-chemistry-climate model ECHAM5-HAMMOZ to quantify the impacts of heterogeneous reactions on the global distributions, compositions, and optical properties of aerosols. The aerosol simulation was first evaluated using a variety of data set, including sulfate and SO_2 surface concentrations measured by the EMEP network (over Europe, Figures S3 and S4 of the auxiliary material), sulfate, black and organic carbon concentrations measured by the IMPROVE network (over the U.S., Figures S5 and S6 of the auxiliary material), and aerosol optical depths provided by the AERONET network at various sites over the world (Figure S7 and Table S1 of the auxiliary material). A good agreement between observed and simulated sulfate concentrations is found in general, but SO_2 concentrations are largely overestimated over Europe. This overestimate can be partly due to too low deposition [*Stier et al.*, 2006], too high emission levels [*de Meij et al.*, 2006] and to a low SO_2 uptake on aerosols (see section 2 in the auxiliary material). The black carbon and organic carbon concentrations show a good agreement over the U.S. with a correlation coefficient of 0.62 and 0.76 and relatively low mean absolute biases, 40% and 26%, respectively. The simulated aerosol optical depths compare well with observations at many sites of the AERONET network, both in terms of annual means and seasonal variations.

[34] In our BASE simulation we find a global burden of 0.77 and 0.87 (Tg(S)) for SO_2 and sulfate, respectively. Our sulfate burden falls in the range of previous estimates, while the SO_2 burden is higher compared to other studies, as also indicated by the overestimate of observed SO_2 concentrations. The effects of heterogeneous reactions were analyzed

through a series of sensitivity simulations. The impact of these reactions on annual mean aerosol burdens is small in general but significant differences are seen for specific regions and seasons. SO_2 is affected by heterogeneous reactions through different competing processes. The decrease in OH (the main oxidant of SO_2) caused by heterogeneous chemistry [*Pozzoli et al.*, 2008] leads to a reduction in H_2SO_4 and sulfate condensation. On the other hand, SO_2 uptake on mineral dust and sea salt leads to the production of sulfate. The balance between these processes is highly variable over the globe; for example, the SO_2 burden generally increases over source regions of dust by up to 15% and decreases over the oceans in the Southern Hemisphere and at high latitudes in the Northern Hemisphere. The resulting effect of these competing processes on the sulfate distributions is in general small. The SO_2 and sulfate burdens are mainly impacted by heterogeneous reactions on nondust particles, but the sulfate formation on dust plays an important role in determining the mixing state of particles, thus influencing the wet deposition efficiency and the lifetime.

[35] We find that the main sources of sulfate are SO_2 in-cloud oxidation (57%) and condensation of H_2SO_4 (34%). Sulfate formed on sea salt particles is 3.69 Tg(S) a^{-1} (5%), in good agreement with the observation-constrained model study of *Alexander et al.* [2005]. Sulfate formed by heterogeneous uptake of SO_2 on mineral dust contributes only 0.55 Tg(S) a^{-1} (<1%), but is responsible for the coating of mineral dust particles thereby changing their mixing state and hygroscopicity. 300 Tg a^{-1} of dust are transferred by this process from the insoluble to the soluble mixed modes, which represents more than 50% of the total mineral dust emitted per year. The ageing of dust by SO_2 uptake decreases the fraction of hydrophobic dust from 56% to 26%, and decreases the dust global annual mean burden by 5% because of enhanced wet deposition efficiency. The globally averaged burden of black carbon does not change significantly because of the heterogeneous reactions. However, the hydrophobic black carbon mass decreases in the Northern Hemisphere, especially over polluted regions. Over the regions where biomass burning sources emit high loads of carbonaceous aerosols, hydrophobic black carbon mass increases while the hydrophilic black carbon decreases.

[36] The changes in black carbon and dust mixing state exert an important impact on aerosol optical properties and in particular on aerosol absorbing properties. We find small variations in globally and annually averaged aerosol absorption optical depth, but significantly larger differences on a regional and seasonal scale. The aerosol optical depth and aerosol absorption optical depth increase by 10 to 40%, and up to 15%, respectively, during winter (DJF) in the main polluted regions (Europe, eastern U.S., and eastern Asia) because of heterogeneous reactions. The changes in the aerosol mixing state due to heterogeneous reactions and sulfur chemistry also induce reductions up to 20% in aerosol absorption optical depth over remote regions.

[37] Some of the trace gas–aerosol interactions described in this work are still affected by large uncertainties. Further experimental studies are needed to investigate the heterogeneous reaction pathways and to reduce the uncertainty associated with the uptake coefficients in order to improve the description of important processes like dust and black carbon coating. The large number of competing and nonlinear processes that contribute to shape the trace gas and aerosol distributions as well as the aerosol composition, mixing state, and optical properties clearly highlight the need to use a coupled model to achieve a comprehensive and quantitative understanding of the radiative forcing of greenhouse gases and aerosols on climate. These processes are also important to assess the indirect effect of aerosols on climate (e.g., by enhancing CCN concentration), the long range transport of aerosols, the impact of aerosol on air quality, and the impact of aerosol deposition on marine and terrestrial ecosystems.

[38] **Acknowledgments.** This work was supported by the Swiss National Science Foundation under the grants 2100-067979 and 200020-112231. We would like to thank the EMEP network for providing SO_2 and sulfate measurements over Europe, the IMPROVE network for providing aerosol concentration measurements over North America, and the AERONET team for providing the aerosol data used in this investigation.

References

Ackerman, T., and O. Toon (1981), Absorption of visible radiation in atmosphere containing mixtures of absorbing and non-absorbing particles, *Appl. Opt.*, *20*(20), 3661–3668.

Alexander, B., R. J. Park, D. J. Jacob, Q. B. Li, R. M. Yantosca, J. Savarino, C. C. W. Lee, and M. H. Thiemens (2005), Sulfate formation in sea-salt aerosols: Constraints from oxygen isotopes, *J. Geophys. Res.*, *110*, D10307, doi:10.1029/2004JD005659.

Andres, R., and A. Kasgnoc (1998), A time-averaged inventory of subaerial volcanic sulfur emissions, *J. Geophys. Res.*, *103*(D19), 25,251–25,261.

Atkinson, R., L. Baulch, R. Cox, J. Crowley, R. F. Hamson, M. Jenkin, J. Kerr, M. Rossi, and J. Troe (2004), Summary of evaluated kinetic and photochemical data for atmospheric chemistry, technical report, Cambridge Univ., Cambridge, U. K. (Available at http://www.iupac-kinetic.ch.cam.ac.uk/summary/IUPACsumm_web_latest.pdf)

Bauer, S. E., and D. Koch (2005), Impact of heterogeneous sulfate formation at mineral dust surfaces on aerosol loads and radiative forcing in the Goddard Institute for Space Studies general circulation model, *J. Geophys. Res.*, *110*, D17202, doi:10.1029/2005JD005870.

Bauer, S. E., Y. Balkanski, M. Schulz, D. A. Hauglustaine, and F. Dentener (2004), Global modeling of heterogeneous chemistry on mineral aerosol surfaces: Influence on tropospheric ozone chemistry and comparison to observations, *J. Geophys. Res.*, *109*, D02304, doi:10.1029/2003JD003868.

Bell, N., D. Koch, and D. T. Shindell (2005), Impacts of chemistry-aerosol coupling on tropospheric ozone and sulfate simulations in a general circulation model, *J. Geophys. Res.*, *110*, D14305, doi:10.1029/2004JD005538.

Bian, H., and M. Prather (2002), Fast-J2: Accurate simulation of stratospheric photolysis in global chemical models, *J. Atmos. Chem.*, *41*(3), 281–296.

Bian, H., and C. S. Zender (2003), Mineral dust and global tropospheric chemistry: Relative roles of photolysis and heterogeneous uptake, *J. Geophys. Res.*, *108*(D21), 4672, doi:10.1029/2002JD003143.

Chameides, W., and A. Stelson (1992), Aqueous-phase chemical processes in deliquescent sea-salt aerosols: A mechanism that couples the atmospheric cycles of S and sea salt, *J. Geophys. Res.*, *97*(D18), 20,565–20,580.

Chin, M., D. J. Jacob, G. M. Gardner, M. S. Foreman-Fowler, P. A. Spiro, and D. L. Savoie (1996), A global three-dimensional model of tropospheric sulfate, *J. Geophys. Res.*, *101*(D13), 18,667–18,690.

Chylek, P., G. Videen, D. Ngo, R. Pinnick, and J. Klett (1995), Effect of black carbon on the optical-properties and climate forcing of sulfate aerosols, *J. Geophys. Res.*, *100*(D8), 16,325–16,332.

Cofala, J., M. Amann, and R. Mechler (2005), Scenarios of world anthropogenic emissions of air pollutants and methane up to 2030, technical report, Int. Inst. for Appl. Syst. Anal., Laxenburg, Austria. (Available at http://www.iiasa.ac.at/rains/global_emiss/global_emiss.html)

Croft, B., U. Lohmann, and K. von Salzen (2005), Black carbon ageing in the Canadian Centre for Climate Modelling and Analysis Atmospheric General Circulation Model, *Atmos. Chem. Phys.*, *5*, 1931–1949.

de Meij, A., M. Krol, F. Dentener, E. Vignati, C. Cuvelier, and P. Thunis (2006), The sensitivity of aerosol in Europe to two different emission inventories and temporal distribution of emissions, *Atmos. Chem. Phys.*,

6, 4287–4309.
Dentener, F., G. Carmichael, Y. Zhang, J. Lelieveld, and P. Crutzen (1996), Role of mineral aerosol as a reactive surface in the global troposphere, *J. Geophys. Res.*, *101*(D17), 22,869–22,889.
Dentener, F., et al. (2006), Emissions of primary aerosol and precursor gases in the years 2000 and 1750, prescribed data-sets for AEROCOM, *Atmos. Chem. Phys. Disc.*, *6*, 2703–2763.
Feichter, J., E. Kjellstrom, H. Rodhe, F. Dentener, J. Lelieveld, and G. Roelofs (1996), Simulation of the tropospheric sulfur cycle in a global climate model, *Atmos. Environ.*, *30*(10–11), 1693–1707.
Fouquart, Y., and B. Bonnel (1980), Computation of solar heating of the earth's atmosphere: A new parameterization, *Beitr. Phys. Atmos.*, *53*, 35–62.
Ganzeveld, L., and J. Lelieveld (1995), Dry deposition parameterization in a chemistry general circulation model and its influence on the distribution of reactive trace gases, *J. Geophys. Res.*, *100*(D10), 20,999–21,012.
Ganzeveld, L., J. Lelieveld, and G. Roelofs (1998), A dry deposition parameterization for sulfur oxides in a chemistry and general circulation model, *J. Geophys. Res.*, *103*(D5), 5679–5694.
Ganzeveld, L., J. van Aardenne, T. Butler, M. Lawrence, S. Metzger, P. Stier, P. Zimmermann, and J. Lelieveld (2006), Technical note: Anthropogenic and natural offline emissions and the online Emissions and Dry Deposition submodel EMDEP of the Modular Earth Submodel System (MESSy), *Atmos. Chem. Phys. Disc.*, *6*, 5457–5483.
Grewe, V., D. Brunner, M. Dameris, J. L. Grenfell, R. Hein, D. Shindell, and J. Staehelin (2001), Origin and variability of upper tropospheric nitrogen oxides and ozone at northern mid-latitudes, *Atmos. Environ.*, *35*(20), 3421–3433.
Grewe, V., M. Dameris, C. Fichter, and D. Lee (2002), Impact of aircraft NOx emissions. part 2: Effects of lowering the flight altitude, *Meteorol. Z.*, *11*(3), 197–205.
Guenther, A., et al. (1995), A global-model of natural volatile organic-compound emissions, *J. Geophys. Res.*, *100*(D5), 8873–8892.
Hallquist, M., D. Stewart, S. Stephenson, and R. Cox (2003), Hydrolysis of N_2O_5 on sub-micron sulfate aerosols, *Phys. Chem. Chem. Phys.*, *5*(16), 3453–3463.
Halmer, M., H. Schmincke, and H. Graf (2002), The annual volcanic gas input into the atmosphere, in particular into the stratosphere: A global data set for the past 100 years, *J. Volcanol. Geotherm. Res.*, *115*(3–4), 511–528.
Horowitz, L. W., et al. (2003), A global simulation of tropospheric ozone and related tracers: Description and evaluation of MOZART, version 2, *J. Geophys. Res.*, *108*(D24), 4784, doi:10.1029/2002JD002853.
Jacob, D. (2000), Heterogeneous chemistry and tropospheric ozone, *Atmos. Environ.*, *34*(12–14), 2131–2159.
Jacobson, M. (2000), A physically-based treatment of elemental carbon optics: Implications for global direct forcing of aerosols, *Geophys. Res. Lett.*, *27*(2), 217–220.
Jeuken, A., P. Siegmund, L. Heijboer, J. Feichter, and L. Bengtsson (1996), On the potential of assimilating meteorological analyses in a global climate model for the purpose of model validation, *J. Geophys. Res.*, *101*(D12), 16,939–16,950.
Kane, S., F. Caloz, and M. Leu (2001), Heterogeneous uptake of gaseous N_2O_5 by (NH_4) (2)SO_4, NH_4HSO_4, and H_2SO_4 aerosols, *J. Phys. Chem. A*, *105*(26), 6465–6470.
Kettle, A., and M. Andreae (2000), Flux of dimethylsulfide from the oceans: A comparison of updated data seas and flux models, *J. Geophys. Res.*, *105*(D22), 26,793–26,808.
Koch, D. (2001), Transport and direct radiative forcing of carbonaceous and sulfate aerosols in the GISS GCM, *J. Geophys. Res.*, *106*(D17), 20,311–20,332.
Langner, J., and H. Rodhe (1991), A global 3-dimensional model of the tropospheric sulfur cycle, *J. Atmos. Chem.*, *13*(3), 225–263.
Liao, H., and J. H. Seinfeld (2005), Global impacts of gas-phase chemistry-aerosol interactions on direct radiative forcing by anthropogenic aerosols and ozone, *J. Geophys. Res.*, *110*, D18208, doi:10.1029/2005JD005907.
Liao, H., P. J. Adams, S. H. Chung, J. H. Seinfeld, L. J. Mickley, and D. J. Jacob (2003), Interactions between tropospheric chemistry and aerosols in a unified general circulation model, *J. Geophys. Res.*, *108*(D1), 4001, doi:10.1029/2001JD001260.
Liao, H., J. H. Seinfeld, P. J. Adams, and L. J. Mickley (2004), Global radiative forcing of coupled tropospheric ozone and aerosols in a unified general circulation model, *J. Geophys. Res.*, *109*, D16207, doi:10.1029/2003JD004456. (Correction, *J. Geophys. Res.*, 109, D24204, doi:10.1029/2004JD005476, 2004.).
Lin, S., and R. Rood (1996), Multidimensional flux-form semi-Lagrangian transport schemes, *Mon. Weather Rev.*, *124*(9), 2046–2070.
Lohmann, U., and E. Roeckner (1996), Design and performance of a new cloud microphysics scheme developed for the ECHAM general circulation model, *Clim. Dyn.*, *12*(8), 557–572.
Lohmann, U., K. von Salzen, N. McFarlane, H. Leighton, and J. Feichter (1999), Tropospheric sulfur cycle in the Canadian general circulation model, *J. Geophys. Res.*, *104*(D21), 26,833–26,858.
Maahs, H. (1983), Kinetics and mechanism of the oxidation of S (IV) by ozone in aqueous-solution with particular reference to SO_2 conversion in nonurban tropospheric clouds, *J. Geophys. Res.*, *88*, 721–732.
Martin, R., D. Jacob, R. Yantosca, M. Chin, and P. Ginoux (2003), Global and regional decreases in tropospheric oxidants from photochemical effects of aerosols, *J. Geophys. Res.*, *108*(D3), 4097, doi:10.1029/2002JD002622.
Mlawer, E., S. Taubman, P. Brown, M. Iacono, and S. Clough (1997), Radiative transfer for inhomogeneous atmospheres: RRTM, a validated correlated-k model for the longwave, *J. Geophys. Res.*, *102*(D14), 16,663–16,682.
Morcrette, J., S. Clough, E. Mlawer, and M. Iacono (1998), Impact of a validated radiative transfer scheme, RRTM, on the ECMWF model climate and 10-day forecasts, *Tech. Rep. 252*, Eur. Cent. for Med.-Range Weather Forecasts, Reading, U. K.
Nightingale, P., G. Malin, C. Law, A. Watson, P. Liss, M. Liddicoat, J. Boutin, and R. Upstill-Goddard (2000), In situ evaluation of air-sea gas exchange parameterizations using novel conservative and volatile tracers, *Global Biogeochem. Cycles*, *14*(1), 373–387.
Nordeng, T. (1994), Extended versions of the convective parameterization scheme at ECMWF and their impact on the mean and transient activity of the model in the tropics, *Tech. Rep. 206*, Eur. Cent. for Med.-Range Weather Forecasts, Reading, U. K.
Pham, M., J. Muller, G. Brasseur, C. Granier, and G. Megie (1995), A three-dimensional study of the tropospheric sulfur cycle, *J. Geophys. Res.*, *100*(D12), 26,061–26,092.
Pozzoli, L. (2007), Climate and chemistry interactions: Develpoment and evaluation of a coupled chemistry-aerosol-climate model, Ph.D. thesis, Ecole Polytech. Fed. de Lausanne, Lausanne, Switzerland.
Pozzoli, L., I. Bey, J. Rast, M. Schultz, P. Stier, and J. Feichter (2008), Trace gas and aerosol interactions in the fully coupled model of chemistry-aerosol-climate ECHAM5-HAMMOZ: 1. Model description and insights from the spring 2001 TRACE-P experiment, *J. Geophys. Res.*, doi:10.1029/2007JD009007, in press.
Rasch, P., M. Barth, J. Kiehl, S. Schwartz, and C. Benkovitz (2000), A description of the global sulfur cycle and its controlling processes in the National Center for Atmospheric Research Community Climate Model, version 3, *J. Geophys. Res.*, *105*(D1), 1367–1385.
Riemer, N., H. Vogel, and B. Vogel (2004), Soot aging time scales in polluted regions during day and night, *Atmos. Chem. Phys.*, *4*, 1885–1893.
Roeckner, E. et al. (2003), The atmospheric general circulation model ECHAM5: Part 1, *Tech. Rep. 349*, Max Planck Inst. for Meteorol., Hamburg, Germany.
Roelofs, G., J. Lelieveld, and L. Ganzeveld (1998), Simulation of global sulfate distribution and the influence on effective cloud drop radii with a coupled photochemistry sulfur cycle model, *Tellus, Ser. B*, *50*(3), 224–242.
Sander, S. et al. (2003), Chemical kinetics and photochemical data for use in atmospheric studies, evaluation number 14, *JPL Publ. 02-25*, Jet Propul. Lab., Calif., Inst. of Technol., Pasadena. (Available at http://jpldataeval.jpl.nasa.gov/pdf/JPL_02-25_rev02.pdf).
Schultz, M., A. Heil, J. Hoelzemann, A. Spessa, K. Thonicke, J. Goldammer, A. Held, J. Pereira, and M. van het Bolscher (2008), Global wildland fire emissions from 1960 to 2000, *Global Biogeochem. Cycles*, doi:10.1029/2007GB003031, in press.
Schulz, M., G. de Leeuw, and Y. Balkanski (2004), Sea-salt aerosol source functions and emissions, in *Emissions of Atmospheric Trace Compounds*, pp. 333–359, Springer, New York.
Simmons, A., D. Burridge, M. Jarraud, C. Girard, and W. Wergen (1989), The ECMWF medium-range prediction models development of the numerical formulations and the impact of increased resolution, *Meteorol. Atmos. Phys.*, *40*(1–3), 28–60.
Song, C., and G. Carmichael (2001), A three-dimensional modeling investigation of the evolution processes of dust and sea-salt particles in east Asia, *J. Geophys. Res.*, *106*(D16), 18,131–18,154.
Stier, P., et al. (2005), The aerosol-climate model ECHAM5-HAM, *Atmos. Chem. Phys.*, *5*, 1125–1156.
Stier, P., J. H. Seinfeld, S. Kinne, J. Feichter, and O. Boucher (2006), Impact of nonabsorbing anthropogenic aerosols on clear-sky atmospheric absorption, *J. Geophys. Res.*, *111*, D18201, doi:10.1029/2006JD007147.
Tegen, I., S. P. Harrison, K. Kohfeld, I. C. Prentice, M. Coe, and M. Heimann (2002), Impact of vegetation and preferential source areas on global dust aerosol: Results from a model study, *J. Geophys. Res.*, *107*(D21), 4576, doi:10.1029/2001JD000963.
Thornton, J., C. Braban, and J. Abbatt (2003), N_2O_5 hydrolysis on sub-micron organic aerosols: The effect of relative humidity, particle phase, and particle size, *Phys. Chem. Chem. Phys.*, *5*(20), 4593–4603.
Tie, X., S. Madronich, S. Walters, D. P. Edwards, P. Ginoux, N. Mahowald, R. Zhang, C. Lou, and G. Brasseur (2005), Assessment of the global impact of aerosols on tropospheric oxidants, *J. Geophys. Res.*, *110*,

D03204, doi:10.1029/2004JD005359.
Tiedtke, M. (1989), A comprehensive mass flux scheme for cumulus parameterization in large-scale models, *Mon. Weather Rev.*, *117*(8), 1779–1800.
Tompkins, A. (2002), A prognostic parameterization for the subgrid-scale variability of water vapor and clouds in large-scale models and its use to diagnose cloud cover, *J. Atmos. Sci.*, *59*(12), 1917–1942.
Toon, O., and T. Ackerman (1981), Algorithms for the calculation of scattering by stratified spheres, *Appl. Opt.*, *20*(20), 3657–3660.
Ullerstam, M., R. Vogt, S. Langer, and E. Ljungstrom (2002), The kinetics and mechanism of SO_2 oxidation by O-3 on mineral dust, *Phys. Chem. Chem. Phys.*, *4*(19), 4694–4699.
Ullerstam, M., M. Johnson, R. Vogt, and E. Ljungstrom (2003), Drifts and Knudsen cell study of the heterogeneous reactivity of SO_2 and NO_2 on mineral dust, *Atmos. Chem. Phys.*, *3*, 2043–2051.
Usher, C. R., H. Al-Hosney, S. Carlos-Cuellar, and V. H. Grassian (2002), A laboratory study of the heterogeneous uptake and oxidation of sulfur dioxide on mineral dust particles, *J. Geophys. Res.*, *107*(D23), 4713, doi:10.1029/2002JD002051.
Usher, C., A. Michel, and V. Grassian (2003), Reactions on mineral dust, *Chem. Rev.*, *103*(12), 4883–4939.
van der Werf, G., J. Randerson, G. Collatz, and L. Giglio (2003), Carbon emissions from fires in tropical and subtropical ecosystems, *Global Change Biol.*, *9*(4), 547–562.
Vignati, E., J. Wilson, and P. Stier (2004), M7: An efficient size-resolved aerosol microphysics module for large-scale aerosol transport models, *J. Geophys. Res.*, *109*, D22202, doi:10.1029/2003JD004485.

I. Bey, Laboratoire de Modélisation de la Chimie Atmosphérique, École Polytechnique Fédérale de Lausanne, Station 2, Lausanne CH-1015, Switzerland.
J. Feichter, L. Pozzoli, and S. Rast, Atmosphere in Earth System, Max Planck Institute for Meteorology, Hamburg D-20146, Germany. (luca.pozzoli@epfl.ch)
M. G. Schultz, Institute of Chemistry and Dynamics of the Geosphere: Troposphere, Forschungzentrum, Jülich D-52425, Germany.
P. Stier, Atmospheric, Oceanic and Planetary Physics, University of Oxford, Oxford OX1 3PU, UK.